Sensor based on *b*-NiO_x hybrid film/multi-walled carbon nanotubes composite electrode for groundwater salinization inspection

Mônica L.M. Firmino [a], Simone Morais [b], Adriana N. Correia [c], Pedro de Lima-Neto [c], Francisco A.O. Carvalho [d], Suely S.L. Castro [a], Thiago M.B.F. Oliveira [a,d,⇑]

[a] *GELQA, Departamento de Química, Universidade do Estado do Rio Grande do Norte, Campus Central, Setor II, 59625-620 Mossoró, RN, Brazil*

[b] *REQUIMTE–LAQV, Instituto Superior de Engenharia do Porto, Instituto Politécnico do Porto, Rua Dr. Bernardino de Almeida 431, 4200-072 Porto, Portugal*

[c] *GELCORR, Departamento de Química Analítica e Físico-Química, Centro de Ciências, Universidade Federal do Ceará, Bloco 940, Campus do Pici, 60440-900 Fortaleza, CE, Brazil*

[d] *GENorB, Faculdade de Química, Instituto de Ciências Exatas, Universidade Federal do Sul e Sudeste do Pará, Folha 17, Quadra 04, Lote Especial, Nova Marabá, 68505-080 Marabá, PA, Brazil*

Abstract

The enrichment of groundwater with different nutrients (Na^+, Ca^{2+}, Mg^{2+}, Cl^-, CO_3^{2-}, among others) triggers the salinization of the aquifer and makes it inappropriate for many purposes. In this work, we developed a highly sensitive and selective electrochemical sensor, based on *Ni*-inorganic films electrosynthetized *in situ* onto multi-walled carbon nanotubes composite paste electrode (MWCNE), which allows the early detection of salinization. The working sensor (*β*-NiO_x/MWCNE) was derivatized from nickel hexacyanoferrate modified electrode in strong alkaline medium (pH = 12), producing a hybrid film composed by *β*-$Ni(OH)_2$and *β*-*NiO*(*OH*). The electrochemical properties, morphology and chemical composition of the formed *β*-NiO_x thin films were evaluated by voltammetry, scanning electron microscopy and X-ray spectroscopy. The developed *β*-NiO_x/MWCNE sensor was highly sensitive to the presence of Na^+ cation by ion-exchange, and the increase of Na^+ concentration in the range 4.46×10^{-7} to 4.93×10^{-6} mol L^{-1} inhibited linearly the reversible electrochemical signal of the device, allowing to determine trace concentrations of this ion (LOD = 9.86×10^{-8} mol L^{-1}) with high correlation coefficient of the data (r = 0.999) and suitable precision/reproducibility of the measurements (RSD < 9%). Using Na^+as salinization marker and *β*-NiO_x/MWCNE as electroanalytical device, we found evidences of groundwater salinization in Grossos, a Brazil coast city, whose inhabitants have hypertension above the national average. The attained results were comparable to those obtained by the standard methods for Na^+ analysis (percentage error ranging from 0.5 to 1.6%), confirming the accuracy of the proposed electroanalytical platform.

Keywords

Groundwater salinizationSodium cationNickel thin filmsIon-exchangeElectrochemical sensor

1. Introduction

Groundwater is the most important natural drinking-water supply of the population and thus, all possible actions of monitor- ing, preservation and sustainable use of this finite resource should be investigated [1–4]. Unfortunately, groundwater reserves are very susceptible to contamination by natural (saline intrusion; leaching of contaminated areas by rainfall action; chemical trans- formation and dissolution of minerals contained in the aquifer rock formation) and/or anthropogenic events (improper disposal of solid and liquid wastewaters from industrial, commercial and domestic activities; leaks of sewage from cesspools built improp- erly; leaching by irrigation of agricultural areas; among others), limiting groundwater multiple use [1,5]. The joint effects of these factors with the extended period of drought in semi-arid zones may worsen the groundwater quality, especially by salinization processes [1,4,6].

Salinization, which constitutes one of the major threats to ecosystems, occurs by the increase of total dissolved solids concen- tration in a certain water or soil matrix, due to the enrichment with different nutrients. So, the accumulation of salts by natural pro- cesses can induces a primary groundwater salinization, but it can also be triggered or worsened by anthropogenic secondary pro- cesses [5,6]. In the context of groundwater, according to geochem- ical and geophysical characteristics of the aquifer, several ions analyze this cation in human urine samples with a detection limit (LOD) of 3.43×10^{-5} mol L^{-1}. Posteriorly, Machini et al. [29] devel- oped a more sensitive Na^+ sensor, employing a carbon paste elec- trode modified with a different manganese oxide (hausmannite- type; 20%; w/w), that reached a LOD of 7.50×10^{-6} mol L^{-1} in the same type of samples. Inorganic thin films exhibit excellent properties for the sensing of alkali metals [32–34], but little atten- tion has been given to Na^+ [29,30]. In addition, no information was found regarding the application of inorganic thin film sensors to Na^+ impacted environmental samples.

Considering that surface-modified electrodes based on NiO_X- films [i.e., *a*-$Ni(OH)_2$, *b*-$Ni(OH)_2$, *b*-*NiO*(*OH*)and *c*-*NiO*(*OH*)] are

interesting zeolitic platform to quantify inorganic nutrients (by ion-exchange process induced electrochemically with high rate of heterogenous electron transfer [32–34]), in this work, a novel and sensitive sensor for Na^+ was architected by using a NiO_X- hybrid film electrosynthetized onto a multi-walled carbon nan- otube composite electrode. The morphology, composition and sta- bility of the NiO_X-film, the detection mechanism and kinetic of mass transport on the sensor/solution interface, as well as the sen- sitivity of the proposed approach were also characterized and com- pared with standard analytical methods for Na^+ quantification. The developed sensor was successfully applied to monitor Na^+ and the consequent salinization process in groundwaters from a seaside town in Brazil coast (Grossos, in Rio Grande do Norte state). This

(Na^+, Ca^{2+}, Mg^{2+}, Cl^-, Br^-, HCO_3 , CO_3 and SO_4) and/or their ratios

(Na^+/Cl^-, Ca^{2+}/Na^+, Mg^{2+}/Ca^{2+}, Br^-/Cl^-, $\bar{C}l^-/HCO_3$, among others) can be used as markers or representative proxies of this phe- nomenon [5,7]. However, considering that sodium is the sixth most abundant element in the Earth's crust and its high reactivity to form ionic compounds, Na^+ content measurements provide direct information about the salinization (and sodification) processes [8,9]. In addition, Na^+ cation is found in virtually all foods and drinking-waters, and its control in the daily diet becomes even more important [10]. Overdoses of sodium in diet have been related to many pathologies and death in several physiological studies with humans and other mammals used as test subjects [11–14]. The American Heart Association warned that hyperten- sion (a chronic disease resulting from high levels of blood pressure in the arteries) causes the largest number of consultations in the public and private health systems, with very important health, eco- nomic and social impacts [15]. Many studies have reported the relation between high levels of Na^+ in drinking- water with the increased blood pressure [16–18], showing the importance of its strict control and monitoring in daily diet, since the prevention is the most cautionary alternative.

Sodium content in complex matrices has been traditionally ana- lyzed by instrumental methods such as flame photometry [19], inductively-coupled plasma spectroscopy [20], atomic absorp- tion/emission spectroscopy [21] and ion chromatography [22], although these techniques require high investment and cannot be applied to *in situ* measurements due to their operational com- plexity. Some researchers have also emphasized the potential of electrochemical methods for Na^+ sensing in aqueous medium, especially using potentiometric measurements based on ion- selective electrodes [23–26]. More robust conductivity sensors have also been proposed for the soil salinity analysis, based on the dielectric properties of the matrix [27]. Promising results have also been obtained with bare and modified amperometric elec- trodes, which allow to analyze different species that impact the environment and the health of dependent organisms, even at very low concentrations [28–31]. Unfortunately, few reports were focused on Na^+ electroanalysis, reinforcing the need for novel elec- trochemical devices for this purpose. Martinez et al. [30] reported a Na^+ sensor structured with carbon paste electrode modified with layered birnessite-type manganese oxide (15%; w/w) and used to city has indicators of patients and victims of hypertension above the national average (around 70% of the number of deaths recorded in the city annually) and there is a supposed relation of these num- bers with the consumption of salinized and/or sodificated drinking-water.

2. Experimental

2.1. *Reagents*

Alkali and alkaline-earth metal salts and hydroxides, including sodium chloride used for the preparation of the standard solutions were purchased from Sigma-Aldrich (Germany). Potassium ferro- cyanide and nickel chloride (Merck, Germany) were used in the electrosynthesis of *Ni*-films on multi-walled carbon nanotubes composite electrode. All chemicals were reagent grade and used without further purification. Ultrapure water (q = 18 MO cm^{-1}) obtained from a PurelabMilli-Q apparatus (Analítica, Brazil) was employed to prepare the solutions.

2.2. *Preparation of the electrochemical sensor*

A multi-walled carbon nanotubes composite electrode (MWCNE) was used as support for the electrosynthesis of *Ni*-films. MWCNE was prepared by mixing multi-walled carbon nan- otubes, average diameter of 10 nm and an average length of 1.5 mm, purified to more than 95% C (DropSens, Spain); graphite powder with – 100 mesh and purity of 99.9% (Ultra Carbon, USA), and paraffin oil binder (Sigma-Aldrich, Germany) in a ratio of 40:50:10% (w/w/w), respectively. The resultant composite was carefully hand-mixed in a mortar and then packed into a cavity of a Teflon® tube (1.0 mm internal diameter) fitted with a stainless steel piston for transduction of the electrical signal. The surface was smoothed against a plain white paper while a slight manual pressure was applied to the piston, and rinsed carefully with ultra- pure water prior each measurement.

The proposed electrochemical sensor was constructed on potentiometric mode, through the immersion of MWCNE in a mixed solution of potassium ferrocyanide (1.0 × 10−3 mol L−1), nickel chloride (1.0 × 10−3 mol L−1) and potassium chloride (0.1 mol L−1), followed by application of a potential variation from 0.0 to 1.0 V (vs. Ag/AgCl/Cl−sat) using cyclic voltammetry (CV; 50 mV s−1) for consecutive scans. This was the first step of the modification, where MWCNE was coated with nickel hexacyanoferrate layers (Ni-HCF), producing the Ni-HCF/MWCNE sensor. Posteriorly, new scans were performed with Ni-HCF/MWCNE in sodium hydroxide (0.01 mol L−1) from 0.0 to 0.7 V (vs. Ag/AgCl/Cl−sat), and Ni-HCF was derivatized in situ into a β-NiOx hybrid film, generating the β-NiOx/MWCNE working sensor.

2.3. Instrumentation

2.4.

MWCNE modification was performed and characterized by voltammetric techniques (CV and square-wave voltammetry (SWV)) using a μ-Autolab Type III electrochemical system (Metrohm Autolab, The Netherlands) fitted with NOVA 1.10 software. The electrochemical cell was assembled with a conventional three-electrode system: β-NiOx/MWCNE as working electrode, a platinum wire as counter electrode, and a Ag/AgCl/Cl−sat (3.0 mol L−1 KCl) as reference electrode. The morphology, metallic composition and crystallinity of Ni-HCF and NiOx inorganic films were also evaluated by high-resolution scanning electron microscopy (SEM; MEV-FEG TESCAN Mira3 LMU, Czech Republic) coupled to energy dispersive X-ray spectroscopy (EDS; Oxford X-ACT diffraction instrument, UK). Elemental composition of the disaggregated electrode materials was also studied by X-ray diffraction – XRD (Rigaku Miniflex-II diffractometer, USA), using Cu Kα1 radiation (λ = 0.154 nm) at 40 kV and 15 mA; graphite monochromator operating at scan rate of 0.02 min−1; and diffraction range of 5–100°. The accuracy and precision of the proposed electroanalytical procedure were compared to standard methods, such as Atomic Absorption Spectroscopy – AAS (Atomic Absorption Spectrometer AA50, Varian – Germany) and Direct Potentiometry – DP (Orion 5-Star Plusmulti-parameter probe, Thermo Scientific – USA) using (Na+)-ion selective electrode.

2.4. Electroanalytical experiments

Qualitative information about pH of the medium, kinetic properties, voltammetric profile and mass transport at electrode/solution interface was obtained by CV. Na+ electroanalysis with the developed β-NiOx/MWCNE sensor and the inspection of the salinization process in groundwater were evaluated by SWV, after optimizing the critical parameters that control the electrochemical signal in this technique, i.e., the frequency (f), pulse amplitude (a) and the height of the potential step (ΔEs). The optimization was based on maximum value of peak current (Ip), displacement of the potential peak (Ep), and alterations on half-peak width (ΔEp/2). All experiments were performed at room temperature (25 °C).

2.5. Na+ quantification and data handling

The targeted cation was indirectly quantified by measuring the inhibition of the anodic signal registered by the β-NiOx/MWCNE sensor in electrolyte solution (0.01 mol L−1 NaOH). An initial current base signal (Io) was firstly measured and then, as the Na+ concentration was increased in the cell, the respective signals (I) were registered being all smaller than Io. Since the diminution of the observed peak current (Ip) was proportional to the concentration of the inhibitor, analytical curves were built for the indirect quantification of Na+ in the range of 4.46 × 10−7 to 4.93 × 10−6 mol L−1. The inhibition percentage (IP, %) was calculated from the following equation:

$$\%IP = \left[1 - \left(\frac{I}{I0}\right)\right] \times 100 \quad (1)$$

The standard deviation of the intercepts and the average of slopes of the straight lines from the analytical curves were used to determine the LOD and quantification limit (LOQ) [35]. Precision of the proposed electroanalytical procedure was evaluated by the relative standard deviations (RSD, %) of 10 consecutive determinations (3.07 × 10−6 mol L−1 Na+) performed on the same day (intraday) and on different days (interday). Reproducibility tests were also made through the comparison of the responses obtained with five different built sensors for the same concentration of the analyte (3.07 × 10−6 mol L−1 Na+).

2.5. Application to real samples and interference tests

The proposed β-NiOx/MWCNE sensor was applied to treated and untreated groundwater samples collected in fifteen different sampling points distributed in Grossos city (area equivalent to 126 km2, occupied by more than 9.000,00 inhabitants), located within an important Brazilian seaside region, in Rio Grande do Norte state. No sample pretreatment was done. The interference of other ionic species that also contribute to the salinization of groundwaters (Li+, K+, Ca2+ and Mg2+) was also investigated at

3.07 × 10−6 mol L−1 Na+. All measurements were performed in triplicate.

3. Results and discussion

3.1. Electrosynthesis of the nickel inorganic films

In aqueous solution, the main challenge for the development of Na+ sensors is related with the highly electronegative reduction potential of this cation (E° = −2.70 V), since the water reduction potential occurs before (E° = −1.23 V) and the production of hydrogen becomes thermodynamically more favored [32], [33], [34]. The effective nuclear charge hinders to move valence electrons from alkali metal ions to lower energy levels and, for this reason, alkali metal ions are considered non-electroactive species. This fact instigates the search for advanced materials, which can be used as electrochemical sensing platforms for these cations, such as nickel-based inorganic films.

Thus, we modified the MWCNE surface with Ni-HCF films and the integration of the unique electrical properties of MWCNE with the zeolitic structure of Ni-HCF generated a powerful electroanalytical platform with high ion-exchange capacity. The successful Ni-HCF/MWCNE development was evidenced by a characteristic voltammetric profile with two well-defined reversible redox pairs (Fig. 1A). The two anodic (Peak 1, Ep = 0.49 V; Peak 2, Ep = 0.60 V) and cathodic peaks (Peak 3, Ep = 0.56 V; Peak 4, Ep = 0.46 V) are related to changes of the iron oxidation state in inorganic complex crystalline network [32], [33], [34], as proposed in the following electrochemical reactions:

$$K_2 Ni^{II}[Fe^{II}(CN)_6] \leftrightarrows KNi^{II}[Fe^{III}(CN)_6] + e^- + K^+ \quad (2)$$

$$KNi^{II}_{1.5}[Fe^{II}(CN)_6] \leftrightarrows Ni^{II}_{1.5}[Fe^{III}(CN)_6] + e^- + K^+ \quad (3)$$

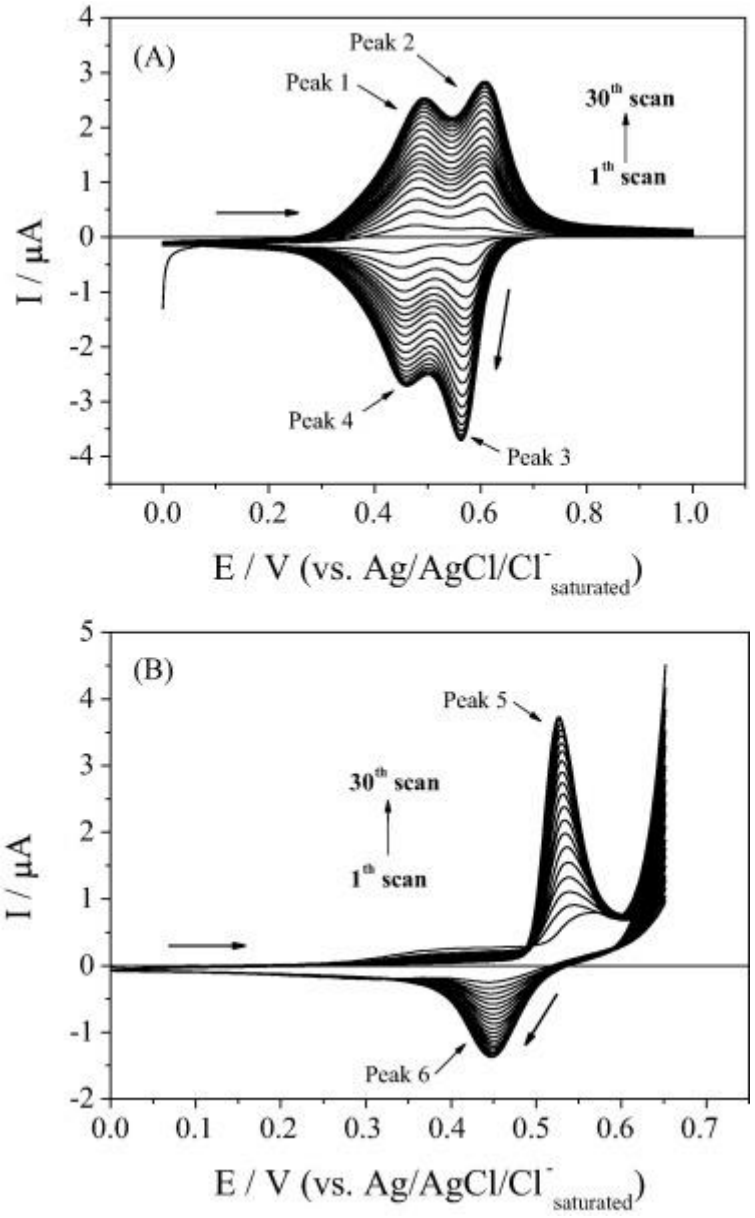

Fig. 1. Electrosynthesis of **(A)***Ni-HCF* and **(B)***NiO_x* hybrid film on MWCNE using cyclic voltammetry at 50 mV s^{-1}.

During the anodic scans, the oxidation of Fe2+ to Fe3+ and release of K+ into the electrolytic solution was observed. Along the cathodic scans, Fe3+ is again reduced to Fe2+, together with the recapture of K+ ions from the bulk solution. The continuous potentiostatic modification through consecutive scans favored a nonlinear increase of the faradaic currents, indicating a significant and favorable decrease of the charge-transfer resistance of the sensor surface. This trend continued until the twentieth cycle remaining constant thereafter (voltammograms overlapped).

NiOx-films were electrosynthetized in situ using Ni-HCF/MWCNE structured with twenty consecutive cyclic scans, in order to facilitate the charge-transfer and increase the signal sensitivity for electroanalytical purposes. After new sequence of consecutive potential scans (0.0–0.7 V; at 50 mV s−1) in 0.01 mol L−1 NaOH solution, a distinct voltammetric profile was observed with two well-defined redox processes (Fig. 1B), which suggested changes in the chemical composition of the Ni-film used as precursor. This fact also gave us the first indication of success on the NiOx electrosynthesis onto the MWCNE surface [33], wherein the anodic (Peak 5; Ep = 0.52 V) and cathodic (Peak 6; Ep = 0.44 V) signals were related with changes of the nickel oxidation states in the as-produced crystalline lattice, as described below:

$$Ni(OH)_2 + OH^- \leftrightarrows NiO(OH) + H_2O + e^- \quad (4)$$

Both Ni(OH)2 and NiO(OH) have a brucite-type unit cell, but with distinct structural varieties based on the lamellar ordering model [36]. These compounds can still be present under different polymorphic structures [i.e., α-Ni(OH)2, β-Ni(OH)2, β-NiO(OH)and γ-NiO(OH)], which may interconvert into the diverse forms according to the charge and discharge processes between the phases, although β-types have a more ordered arrangement along the crystallographic axis. From the sensing point of view, and although β-NiO(OH) orientation is also thermodynamically more stable in alkaline medium, it was still possible to observe a low-intensity redox process (Ep = 0.40 V) at the first potential scan, which probably was due to conversion of γ-NiO(OH) residual amounts to β-NiO(OH). Increasing the number of cycles, the redox processes of β-type compounds became even more intense and defined, until they stabilized after twenty consecutive cyclic scans of potential, justifying the choice of this number of scans for the further experiments. Another important evidence found for this material was its high electrocatalytic activity for the water oxidation, which can be described by the following set of reversible reactions:

$$2\,Ni\,(OH)_2 \leftrightarrows 2\,NiO(OH) + 2H^+ + 2e^- \quad (5)$$

$$4\,NiO(OH) + 2H_2O \leftrightarrows O_2 + 4\,Ni\,(OH)_2 \quad (6)$$

Experimentally, this fact was verified by the highly significant increase of the currents at Ep ≥ 0.6 V along the cycles. Beyond electroanalytical purposes, the mentioned characteristics also enhance the attractive properties of this material for other applications, such as construction of fuel cells, electric batteries, supercapacitors, electrosynthesis, and advanced electrooxidation of toxic and/or refractory substances.

3.2. Characterization of the nickel inorganic films

Before and after each electrochemical modification with Ni-films, the morphological structure of the used materials was investigated by SEM/EDS. The results indicated a highly porous surface for MWCNE (Fig. 2A) that, in turn, facilitates the process of surface sensor modification. It was also possible to observe the complete coverage of the MWCNE surface by the Ni-HCF-precursor film (Fig. 2B), using the experimental conditions mentioned above, showing the efficiency of the electrosynthesis protocol employed to obtain the first Ni-film. Apparently, NiOx/MWCNE (Fig. 2C) and Ni-HCF/MWCNE have a similar superficial morphology, but their lamellar organization and properties are distinct. At a higher magnification level, it can be noticed by a diagonal angle a micro-scaled NiOx grains framework, which were uniformly structured as crystal prisms (±1 μm) on the MWCNE surface (Fig. 2D). EDS mapping showed a relatively uniform and continuous Ni distribution throughout Ni-HCF/MWCNE (Fig. 2E) and NiOx/MWCNE (Fig. 2F) surfaces, indicating appropriate modifications. The small differences in Ni mapping on the films may be related to slight variations of the surface resistivity.

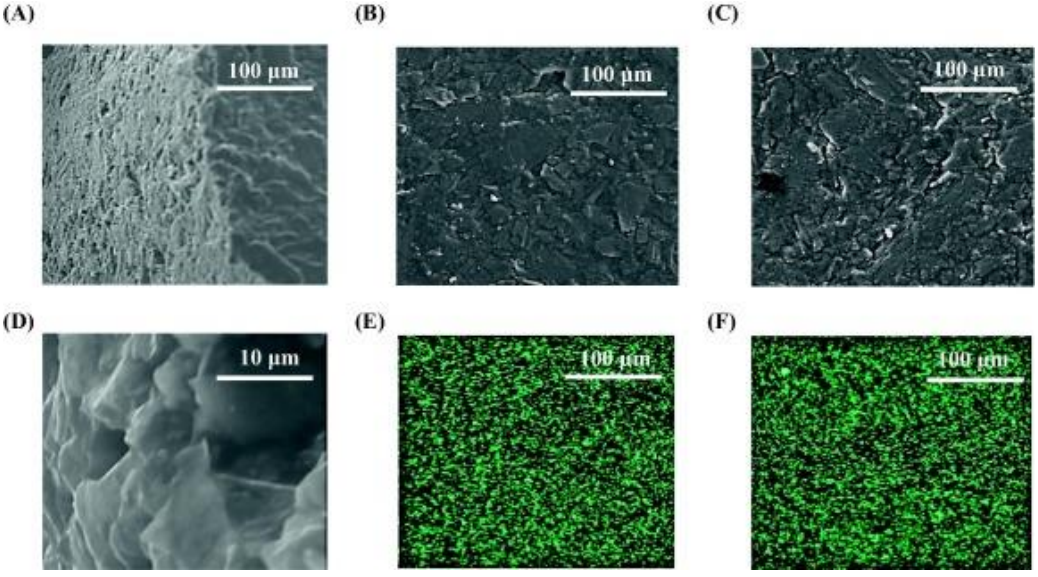

Fig. 2. SEM images of MWCNE (A), Ni-HCF/MWCNE (B) and β-NiOx/MWCNE (C) and (D) (at two different amplifications). EDX mapping of Ni in Ni-HCF/MWCNE (E) and β-NiOx/MWCNE (F).

XRD was used in order to ascertain the quality and crystalline nature of the studied materials. Observing the Fig. 3, we can perceive different diffraction peaks for MWCNE at 2θ equivalent to 26.5°, 42.7°, 44.1° and 77.3°, which were indexed to (0 0 2), (1 0 0), (1 0 1) and (1 1 0) crystallographic planes reflections of the carbonaceous nano-materials (JCPDS cards No. 75-1621 and 26-1077), so that the small downward shift can be attributed to prevalence of sp2 hybridization and CC layers spacing in the nanotube structures [37]. XRD patterns also showed relatively strong diffraction peaks of porous Ni films (2θ = 2θ = 44.1°-(1 1 1), 54.4°-(2 0 0) and 77.3°-(2 2 0); JCPDS No. 04-0850) for both Ni-HCF/MWCNE and NiOx/MWCNE, which reinforce the success of the performed modifications. Regarding the NiOx crystalline structures, the results evidenced characteristic patterns for β-Ni(OH)2[2θ = 15.6°-(0 0 1), 26.5°, 44.1°-(1 0 1), 60.0°-(1 1 0) and 77.3°; JCPDS No. 14-0117], NiO [2θ = 44.1°-(2 0 0), 60.0°-(2 2 0), 77.3°-(3 1 1), 83.1°-(2 2 2) and 86.8°; JCPDS No. 47-1049] and β-NiO(OH) [15.6°-(0 0 1), 26.5°, 44.1°-(0 0 2) and 60.0°-(1 1 0); JCPDS No. 6-0141], which may overlap and support the hypothesis of NiOx-hybrid film electrogenerated in situ. Although the peak widening at 2θ = 15.6°, which indicated a probable α/β-phase transition in the NiOx composition, the combined analysis of the results attained by voltammetry and diffractometry suggested that β-Ni(OH)2 and β-NiO(OH) phases were the most predominant ones [36], [38]. In addition, the narrow and low-intensity peaks of Ni-based compounds compared to the main diffraction signal of the carbonaceous nano-materials (2θ = 26.5°) also attested the very thin thickness and high organization of NiOx-layer [38].

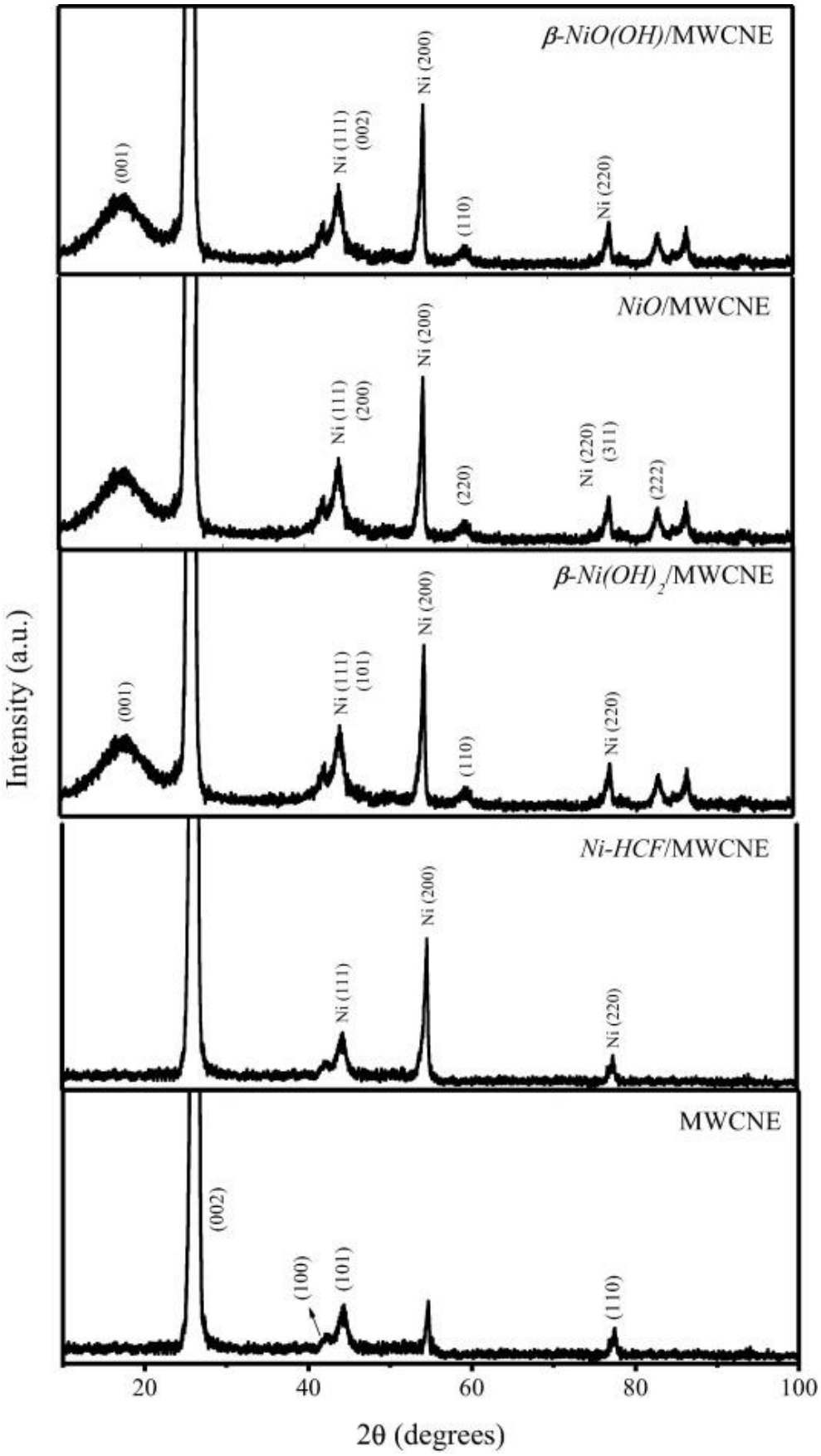

Fig. 3. XRD patterns and crystallographic planes obtained for bare MWCNE, Ni-HCF/MWCNE and β-NiOx/MWCNE modified electrodes.

3.3. Characterization of the sensor stability and process kinetics

β-NiOx/MWCNE sensor, obtained after twenty consecutive potential scans, presented Ep(anodic) = 0.52 V and Ep(cathodic) = 0.44 V, using a scan rate (v) of 50 mV s−1 in 0.01 mol L−1 NaOH. In alkaline medium (pH = 12), this voltammetric profile remained practically constant for more than five hundred consecutive cycles (RSD = 2.3%, n = 5) and over one month (RSD = 7.5%, n = 5), showing high stability of the as-prepared modified sensor. The decrease of the pH impaired the β-NiOx/MWCNE stability and sensitivity, becoming unsuitable in acid medium due to disaggregation of the electrodeposit. However, considering that groundwaters have pH ranging from slightly neutral to alkaline, the sensor functionality is not compromised. Even for samples with acid character, the maintenance of the alkaline medium can be easily guaranteed in the electrochemical cell using the proposed experimental conditions.

Ranging the scan rate (v) from 50 to 500 mV s−1 (Fig. 4A), it was observed a nonlinear increase of Ip values for both anodic and cathodic processes, besides the displacement of Ep(anodic) and Ep(cathodic) to more positive and negative values, respectively. This behavior is characteristic of diffusion-controlled processes and may be related to the relatively slow diffusion of ions into the hydrous crystalline network. Plotting Ip(anodic) and Ip(cathodic) values against the square root of the scan rate (v1/2), the following linear regression Eqs. (7), (8) were reached:

$$I_{p(anodic)}\ [\mu A] = -2.39 + 0.73v^{1/2}\ [(\mathrm{mV\ s^{-1}})^{1/2}] \quad |r = 0.997;\ n = 9| \tag{7}$$

$$I_{p(cathodic)}\ [\mu A] = 1.16 - 0.29v^{1/2}\ [(\mathrm{mV\ s^{-1}})^{1/2}] \quad |r = 0.998;\ n = 9| \tag{8}$$

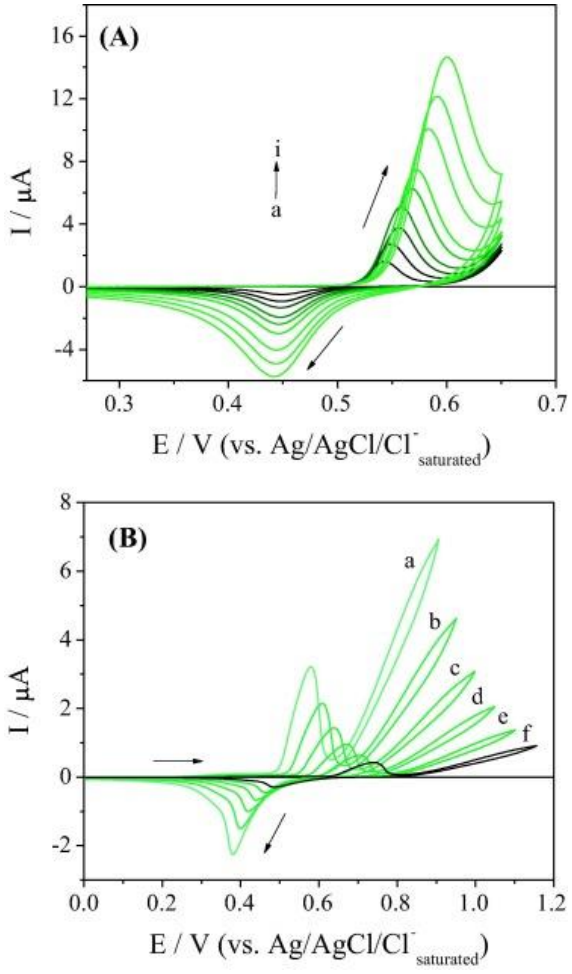

Fig. 4. Cyclic voltammograms obtained with the developed *β*-NiOx/MWCNE sensor **(A)**at different scan rates: (a) 25, (b) 50, (c) 75, (d) 100, (e) 150, (f) 200, (g) 300, (h) 400 and (i) 500 mV s^{-1}; **(B)** at 100 mV s^{-1} after adding (a) 1.0 × 10^{-6}, (b) 5.0 × 10^{-6}, (c) 1.0 × 10^{-5}, (d) 5.0 × 10^{-5} and 1.0 × 10^{-4} mol L^{-1} Na^{+}.

From the variation of Ep(anodic) and Ep(cathodic) values against the logarithm of the scan rate (log v), it is possible to estimate the apparent electrochemical rate constant (ke) and the electron-transfer coefficient (α) for surface redox couples [30]. These relationships can be described by the regression Eqs. (9), (10) presented below:

$$\log v\ [log(\mathrm{mV\ s^{-1}})] = 0.48 + 0.15E_{p(anodic)}\ [V] \quad |r = 0.997;\ n = 9| \tag{9}$$

$$\log v\ [log(\mathrm{mV\ s^{-1}})] = 0.46 - 0.31E_{p(cathodic)}\ [V] \quad |r = 0.998;\ n = 9| \tag{10}$$

It is know that the angular coefficients of the previous relations are equivalent to 2.303RT/(1 − αanodic)nF and −2.303RT/αcathodicnF for the anodic and cathodic processes, respectively, where “R” is the gas constant, “T” is the absolute temperature, “F” is the Faraday constant and “n” is the number of electrons involved in the redox processes. The attained values of αanodic (0.67) and αcathodic (0.19) were further used to estimate the apparent electrochemical rate constant by:

$$k_e = \frac{\alpha_{catodic} nFv^{\circ}}{RT} = (1 - \alpha_{anodic})\frac{nFv^{\circ}}{RT} \tag{11}$$

where the values of are determined by extrapolation of the straight line at high scan rates (200–500 mV s−1). A value of ke = 5.91 s−1 was found indicating fast electronic ion-exchange phenomena at the interface sensor/solution.

Keeping the scan rate constant, it was noticed that β-NiOx/MWCNE and its precursor (Ni-FCF/MWCNE) were sensitive to the presence of Na+ cations. However, the latter was limited to perform tests in neutral medium and showed higher susceptibility to interferences of other alkali and earth-alkali metal ions. Thus, the electrochemical response of β-NiOx/MWCNE to different Na+ concentrations (1.0 × 10−6 to 1.0 × 10−4 mol L−1) was tested by CV at 100 mV s−1, as can be seen in Fig. 4B. In general, the increase of Na+ concentration in the electrolytic cell induced non-linear displacements of Ep(anodic) toward more positive values, while Ep(cathodic) becomes more negative. There was also a pronounced decrease of both Ip(anodic) and Ip(cathodic) intensity. These effects were probably due to alterations of the resistivity in β-NiOx crystalline lattice caused by the ion-exchange processes in order to maintain the charge balance. Larger hydrated ions, such as Na+ (hydrated ionic radius = 2.76 Å; ionic mobility = 43.5 ohm−1 cm2 mol−1), diffuse slowly within the NiOx-film (interlamellar distance ≈ 4.60 Å), intercalating at the interstitial sites and thereby hampering the charge-transfer process [36]. This feature indicated that β-NiOx/MWCNE is a suitable sensor to monitor Na+, even at low concentrations.

3.4. Optimization of electroanalytical parameters

The best analytical signal for Na+ electroanalysis was studied by SWV (since it provides more intense faradaic current signals when compared to CV) after optimizing the critical operational parameters, i.e., the frequency (f; 10–500 s−1), pulse amplitude (a; 5–50 mV) and the height of the potential step (ΔEs; 1–5 mV). It was verified that both anodic and cathodic processes can be used for electroanalytical purposes, but the first one was more intense and reproducible, allowing to improve the sensitivity of the proposed procedure. Using the anodic signal, Ep values displaced toward oxygen production when “f” increased, and there was also a linear relationship between Ip and f until 100 s−1. For f ≥ 150 s−1, a significant increase in signal noise was noted. Regarding “a” selection, a pronounced increase of the half-peak width was detected for a ≥ 30 mV, which can decrease the selectivity of the procedure. Finally concerning the optimization of the scan increment variations, results indicated that ΔEs > 2 mV did not significantly enhance the peak currents. In addition, different preconcentration potentials and times were also investigated, but no significant improvements of the peak intensity were noted. Thus, the optimum SWV conditions for Na+ electroassay on the β-NiOx/MWCNE sensor were selected as being f = 100 s−1, a = 30 mV and ΔEs = 2 mV.

3.5. Na+ quantification and merit figures

Employing the optimized SWV conditions and making successive and standard additions of the analyte, inhibition of the electroanalytical signal of the β-NiOx/MWCNE reached almost 40% of its steady state current in the smallest linear range tested (from 4.46 × 10−7 to 4.93 × 10−6 mol L−1) (Fig. 5A). The following linear regression equation was attained:

$$IP\ (\%) = 4.97 + 6.72 \times 10^{6}\ [Na^{+}]\ (\mathrm{mol\ L^{-1}}) \quad |r = 0.999;\ n = 6| \tag{12}$$

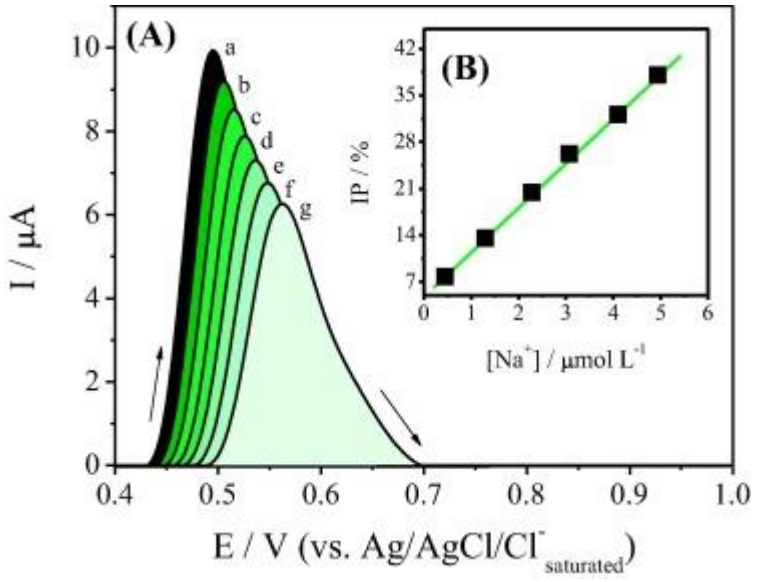

Fig. 5. (A) Square-wave voltammograms of the anodic signal of the β-NiOx/MWCNE sensor using a frequency of 100 s−1, amplitude of 30 mV and potential increments of 2 mV in (a) pure supporting electrolyte and after adding (b) 4.46 × 10−7, (c) 1.29 × 10−6, (d) 2.28 × 10−6, (e) 3.07 × 10−6, (f) 4.09 × 10−6 and (g) 4.93 × 10−6 mol L−1 Na+. (B) Corresponding analytical curve obtained from the inhibition percentage (IP%) of the sensor anodic signal.

The high correlation coefficient indicated low dispersion of the data (Fig. 5B). The standard deviation of the intercepts and the slopes of the straight lines were used to estimate the LOD and LOQ [35], [39]. A LOD = 9.86 × 10−8 mol L−1 (2.27 × 10−3 mg Na+ L−1) and a LOQ = 2.65 × 10−7 mol L−1 (6.09 × 10−3 mg Na+ L−1) were found, emphasizing the high sensitivity of the developed β-NiOx/MWCNE sensor for Na+ quantification. The reached limits are significantly lower than those reported for carbon paste electrode modified with layered birnessite-type manganese oxide (15%, w/w; LOD = 3.43 × 10−5 mol L−1) [30] and hausmannite-type manganese oxide (20%, w/w; LOD = 7.50 × 10−6 mol L−1) [29] in human urine.

The precision of the measurements was established by repeatability experiments (3.07 × 10−6 mol L−1 Na+) performed on the same (intraday) and different days (interday), and low relative standard deviations (RSD < 6.0%) were obtained for both cases. RSD value was slightly higher (RSD = 8.6%) when the reproducibility was tested with five different constructed sensors, but still clearly acceptable.

3.6. Interference studies

The feasibility of application of the β-NiOx/MWCNE sensor for salinization tests in groundwater was assessed using Na+ as marker (3.07 × 10−7 mol L−1) in the presence of different alkaline (Li+ and K+) and earth-alkaline (Mg2+, Ca2+ e Ba2+) metal ions at the same concentration, since they can influence the sensor response due to a similar ion-exchange mechanism (Fig. 6). The results indicated that earth-alkaline metal ions had a minor effect on the Na+ signal (1.0–2.5%), probably due to the formation of insoluble hydroxides of these cations. In a real groundwater sample, by conducting the experiments in strongly alkaline medium, earth-alkaline metal ions could also precipitate as sulphates, carbonates and oxides, further reducing possible interferences. On the other hand, the alkaline metal ions can be intercalated into the β-NiOx film, interfering between 12% (K+) and 25% (Li+) in the Na+ response at the tested concentrations. These findings may be associated to the similar ionic radius of K+ (1.38 Å), or even lower of the Li+ radius (0.76 Å), when compared to Na+ (1.02 Å), which facilitated the reactions of intercalation/deintercalation within the crystalline structure [34], [36], [38]. In groundwaters, these ions are present in trace concentrations and clearly lower than those found for Na+. Thus, it can be considered that K+ and Li+ will not interfere significantly in real groundwater salinity tests.

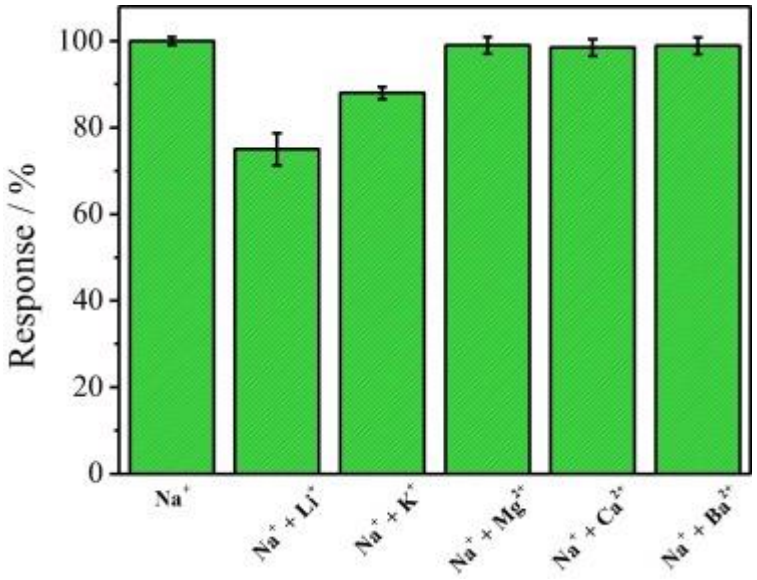

Fig. 6. Effect of selected cationic interferences (Li+, K+, Mg2+, Ca2+ and Ba2+) on the electroanalytical signal of the β-NiOx/MWCNE sensor.

3.7. Electrochemical inspection of groundwater salinization

Direct Na+ electroanalysis was performed by SWV, under the previously optimized experimental conditions (f = 100 s−1, a = 30 mV and ΔEs = 2 mV), in a total of fifteen different treated (twelve sampling points) and untreated (three sampling points) groundwater samples collected in Grossos city, Brazil. This city stands out by the extraction, refining, import and export of sea-salt and other secondary products. Unfortunately, the local population has also experienced chronic problems with hypertension and other related pathologies for many years, exceeding by more than 30% the national average, so that the salinization of groundwater used for human consumption appears as an important issue. In general, the average concentration of Na+ ions detected in treated waters (sequential process of decantation, precipitation and microbiological action) was 100 ± 10 mg L−1, showing evidences of groundwater salinization. However, the most critical situation was identified in untreated waters, where the contents of this nutrient achieved values of 600 ± 13 mg L−1. There are several natural and anthropogenic sources, being the most influential factors the inadequate disposal of highly saline industrial effluents, contamination of soils with industrial by-products, incorrect land management, percolation of contaminated areas, erosion of the constituent rocks of the aquifer, and ocean water intrusion [1], [4], [5], [6], [7], [8], [27]. Still, the attained results also showed a positive impact of the employed conventional treatments, but they seem not yet sufficient to reach the maximum permitted limit (20 mg L−1) established by World Health Organization [10] and United States Environmental Protection Agency [40] for drinking-water.

In order to evaluate the accuracy, the results obtained by the proposed β-NiOx/MWCNE sensor were compared with those achieved by the traditional standard methods: AAS (at 589 nm) coupled with laminar flow burner and DP performed with a (Na+)-ion selective electrode. Low relative errors were observed ranging from 0.5 to 0.9% for AAS and from 0.8 to 1.6% for DP, confirming the reliability of the developed sensing approach. Thus, it can be used for groundwater salinization inspection, which may help to develop efficient strategies to ensure drinking-water quality.

4. Conclusions

The present study proposed a novel β-NiOx/MWCNE sensor for Na+ and salinization monitoring in groundwaters. The most important characteristic of the developed device is the high stability of the in situ electrogenerated Ni-inorganic films, which promote high uniformity of the morphology, crystalline arrangement and appropriate electrokinetic properties. The increase of the Na+ concentration inhibited the redox signal of the sensor (in the 4.46 × 10−7 to 4.93 × 10−6 mol L−1 range; LOD = 9.86 × 10−8 mol L−1 and LOQ = 2.65 × 10−7 mol L−1) due to the diffusion of this cation within the crystalline reticule and increase of the charge-transfer resistance. The achieved performance of the β-NiOx/MWCNE sensor allowed the efficient inspection of salinized groundwater using Na+ as marker. Therefore, the developed electroanalytical platform can be a promising tool to help

controlling the impact of anthropogenic and natural factors, which promote salinization and represent threats to ecosystems in general and water quality in particular. Furthermore, studies are ongoing to test the proposed sensor in other complex and environmentally relevant matrices, such as soils and industrial effluents.

Acknowledgements

The authors are grateful to CNPq (Proc. 400223/2014-7) for the project financing. S. Morais and M.L.M. Firmino also thank for the Scientific Fellowship awarded to them by CNPq (Proc. 303596/2014-7) and FAPERN, respectively.

References

[1]L. Cary, E. Petelet-Giraud, G. Bertrand, W. Kloppmann, L. Aquilina, V. Martins, R.Hirata, S. Montenegro, H. Pauwels, E. Chatton, M. Franzen, A. Aurouet, E.Lasseur, G. Picot, C. Guerrot, C. Fléhoc, T. Labasque, J.G. Santos, A. Paiva, G.Braibant, D. Pierre, Origins and processes of groundwater salinization in theurban coastal aquifers of Recife (Pernambuco, Brazil): a multi-isotopeapproach, Sci. Total Environ. 530–531 (2015) 411–429.

[2]H. Fyles, C. Madramootoo, Water management, in: C. Madramootoo (Ed.),Emerging Technologies for Promoting Food Security: Overcoming the WorldFood Crisis, Woodhead Publishing, Cambridge, 2016, pp. 117–134.

[3]E. Hadz˘ic´, N. Lazovic´, A. Mulaomerovic´-Šeta, The importance of groundwatervulnerability maps in the protection of groundwater sources. Key study:Sarajevsko Polje, Procedia, Environ. Sci. 25 (2015) 104–111.

[4]J. Li, Y. Wang, X. Xie, Cl/Br ratios and chlorine isotope evidences forgroundwater salinization and its impact on groundwater arsenic, fluorideand iodine enrichment in the Datong basin, China, Sci. Total Environ. 544(2016) 158–167.

[5]A. Bouderbala, Groundwater salinization in semi-arid zones: an example fromNador plain (Tipaza, Algeria), Environ. Earth Sci. 73 (2015) 5479–5496.

[6]J.-C. Comte, R. Cassidy, J. Obando, N. Robins, K. Ibrahim, S. Melchioly, I.Mjemah, H. Shauri, A. Bourhane, I. Mohamed, C. Noe, B. Mwega, M. Makokha,J.-L. Join, O. Banton, J. Davies, Challenges in groundwater resourcemanagement in coastal aquifers of East Africa: investigations and lessonslearnt in the Comoros Islands, Kenya and Tanzania, J. Hydrol. 5 (2016) 179–199.

[7]A.B. Moussa, K. Zouari, V. Marc, Hydrochemical and isotope evidence ofgroundwater salinization processes on the coastal plain of Hammamet-Nabeul,north-eastern Tunisia, Phys. Chem. Earth 36 (2011) 167–178.

[8]Y. Mau, A. Porporato, A dynamical system approach to soil salinity andsodicity, Adv. Water Resour. 83 (2015) 68–76.

[9]I.P. Sentís, Advances in the prognosis of soil sodicity under dryland irrigatedconditions, Int. Soil Water Conserv. Res. 2 (2014) 50–63.

[10] WHO – World Health Organization, Sodium in Drinking-Water: BackgroundDocument for Development of WHO Guidelines for Drinking-Water Quality,World Health Organization, Geneva, 2003.

[11]M.H. Alderman, Dietary sodium: where science and policy diverge, Am. J.Hypertens. 29 (2016) 424–427.

[12]K.E. Charlton, K. Lagford, J. Kaldor, Innovative and collaborative strategies toreduce population-wide sodium intake, Curr. Nutr. Rep. 4 (2015) 279–289.

[13]M.H. De Borst, G. Navis, Sodium intake, RAAS-blockade and progressive renaldisease, Pharmacol. Res. 107 (2016) 344–351.

[14]J.W. Hong, J.H. Noh, D.-J. Kim, Factors associated with high sodium intakebased on estimated 24-hour urinary sodium excretion, Medicine 95 (2016)e2864.

[15]D. Lloyd-Jones, R.J. Adams, T.M. Brown, M. Carnethon, S. Dai, G. De Simone, T.B.Ferguson, et al., Heart disease and stroke statistics – update: a report from theAmerican Heart Association, Circulation 121 (2010) (2010) e46–e215.

[16]F.J. He, G.A. MacGregor, Salt intake, sugar-sweetened soft drink consumption,and blood pressure, Am. J. Cardiol. 114 (2014) 499–500.

[17]P.F.D. Scheelbeek, M.A.H. Chowdhury, A. Haines, D.S. Alam, M.A. Hoque, A.P.Butler, A.E. Khan, S.K. Mojumder, M.A.G.

Blangiardo, P. Elliott, P. Vineis, Highconcentrations of sodium in drinking water and raised blood pressure incoastal deltas affected by episodic seawater inundations, Lancet Glob. Health 4(2016) 18;V. Reddy, A. Sridhar, R.F. Machado, J. Chen, High sodium causes hypertension:evidence from clinical trials and animal experiments, J. Integr. Med. 13 (2015)1–8.

[18]M.H. Vingerhoeds, M.A. Nijenhuis-de Vries, N. Ruepert, H. Van der Laan, W.L.P.Bredie, S. Kremer, Sensory quality of drinking water produced by reverseosmosis membrane filtration followed by remineralisation, Water Res. 94(2016) 42–51.

[19]I. Castanheira, C. Figueiredo, C. André, I. Coelho, A.T. Silva, S. Santiago, T.Fontes, C. Mota, M.A. Calhau, Sampling of bread for added sodium asdetermined by flame photometry, Food Chem. 113 (2009) 621–628.

[20]A. Mani-Varnosfaderani, M. Jamshidi, A. Yeganeh, M. Mahmoudi,Concentration profiling of minerals in iliac crest bone tissue of opiumaddicted humans using inductively coupled plasma and discriminantanalysis techniques, J. Pharmaceut. Biomed. 120 (2016) 92–99.

[21]R. Moreno-Rojas, F. Cámara-Martos, M.Á. Amaro López, Sodium: propertiesand determination, in: B. Caballero, P.M. Finglas, F. Toldrá (Eds.), ReferenceModule in Food Science – Encyclopedia of Food and Health, Elsevier, Oxford,2016, pp. 19–23.

[22]L.B. De Caland, E.L.C. Silveira, M. Tubino, Determination of sodium, potassium,calcium and magnesium cations in biodiesel by ion chromatography, Anal.Chim. Acta 718 (2012) 116–120.

[23]A. Jasin´ski, M. Guzin´ski, G. Lisak, J. Bobacka, M. Bochen´ska, Solid-contact lead(II) ion-selective electrodes for potentiometric determination of lead(II) inpresence of high concentrations of Na(I), Cu(II), Cd(II), Zn(II), Ca(II) and Mg(II),Sensors Actuat. B 218 (2015) 25–30.

[24]N.M. Makarova, E.G. Kulapina, New potentiometric screen-printed sensors fordetermination of homologous sodium alkylsulfates, Sensors Actuat. B 210(2015) 817–824.

[25]S.S. Nielsen, Sodium determination using ion selective electrodes, Mohrtitration, and test strips, in: S.S. Nielsen (Ed.), Food Analysis LaboratoryManual, Springer, New York, 2003, pp. 57–66.

[26]L. Parra, S. Sendra, J. Lloret, I. Bosch, Development of a conductivity sensor formonitoring groundwater resources to optimize water management in smartcity environments, Sensors 15 (2015) 20990–21015.

[27]J. Wu, P. Li, H. Qian, Y. Fang, Assessment of soil salinization based on a low-costmethod and its influencing factors in a semi-arid agricultural area, NorthwestChina, Environ. Earth Sci. 71 (2014) 3465–3475.

[28]R. Jain, N. Jadon, K. Singh, Review – new generation electrode materials forsensitive detection, J. Electrochem. Soc. 163 (2016) H159–H170.

[29]W.B.S. Machini, C.S. Martin, M.T. Martinez, S.R. Teixeira, H.M. Gomes, M.F.S.Teixeira, Development of an electrochemical sensor based on nanostructuredhausmannite-type manganese oxide for detection of sodium ions, SensorsActuat. B 181 (2013) 674–680.

[30]M.T. Martinez, A.S. Lima, N. Bocchi, M.F.S. Teixeira, Voltammetric performanceand application of a sensor for sodium ions constructed with layeredbirnessite-type manganese oxide, Talanta 80 (2009) 519–525.

[31]D. Omanovic´, C. Garnier, K. Gibbon-Walsh, I. Piz˘eta, Electroanalysis inenvironmental monitoring: tracking trace metals – a mini review,Electrochem. Commun. 61 (2015) 78–83.

[32]N. Bagkar, C.A. Betty, P.A. Hassan, K. Kahali, J.R. Bellare, J.V. Yakhmi, Self-assembled films of nickel hexacyanoferrate: electrochemical properties andapplication in potassium ion sensing, Thin Solid Films 497 (2006) 259–266.

[33]N. Li, Z. Li, J. Yuan, J. Hu, J. Miao, Q. Zhang, L. Niu, J. Song, Nickelhexacyanoferrate nanoparticles anchored to multiwalled carbon nanotubeswith a grafted poly(4-vinylpyridine) linker for electrically switched ionexchange, Electrochim. Acta 72 (2012) 150–156.

[34]X.-G. Hao, Y.Q.-M. Yu, S.-Y. Jiang, D.T. Schwartz, Molecular dynamicssimulation of ion selectivity traits of nickel hexacyanoferrate thin films,Trans. Nonferr. Metal. Soc. 16 (2006) 897–902.

[35]J.N. Miller, J.C. Miller, Statistics and Chemometrics for Analytical Chemistry,Pearson Prentice Hall, United Kingdom, 2005.

[36]D.S. Hall, D.J. Lockwood, C. Bock, B.R. MacDougall, Nickel hydroxides andrelated materials: a review of their structures, synthesis and properties, Proc.Math. Phys. Eng. Sci. 471 (2015) 1–65.

[37]V. Gupta, T. Saleh, Synthesis of carbon nanotube-metal oxides composites;adsorption and photo-degradation, in: S. Bianco (Ed.), Carbon Nanotubes –From Research to Applications, Intech, Rijeka, 2011, pp. 295–312.

[38]H. Jiang, Y. Guo, T. Wang, P.-L. Zhu, S. Yu, Y. Yu, X.-Z. Fu, R. Sun, C.-P. Wong,Electrochemical fabrication of Ni(OH)2/Ni 3Dporous composite films asintegrated capacitive electrodes, RSC Adv. 5 (2015) 12931–12936.

[39]T.M.B.F. Oliveira, F.W.P. Ribeiro, J.M. Do Nascimento, J.E.S. Soares, V.N. Freire,H. Becker, P. De Lima-Neto, A.N. Correia, Direct electrochemical analysis ofdexamethasone endocrine disruptor in raw natural waters, J. Braz. Chem. Soc.23 (2012) 110–119.

[40] USEPA – United States Environmental Protection Agency, Drinking wateradvisory: consumer acceptability advice and health effects analysis on sodium,U.S. Environmental Protection Agency Office of Water and Health andEcological Criteria Division Washington, 2003.